Adhesion Property Profiles of Supported Thin Polymer Films

Bizan N. Balzer,[†] Samantha Micciulla,[‡] Samuel Dodoo,[‡,||] Maximilian Zerball,[‡] Markus Gallei,[§] Matthias Rehahn,[§] Regine v. Klitzing,[‡] and Thorsten Hugel*[,†]

[†]IMETUM and Physik-Department, Technische Universität München, Boltzmannstr.11, 85748 Garching, Germany
[‡]Stranski-Laboratorium, Institut für Chemie, Technische Universität Berlin, Straße des 17. Juni 124, 10623 Berlin, Germany
[§]Ernst-Berl Institut für Makromolekulare Chemie, Technische Universität Darmstadt, Petersenstraße 22, 64287 Darmstadt, Germany

S *Supporting Information*

ABSTRACT: Polymer coatings are frequently utilized to control and modify substrate properties. The performance of the coatings is often determined by the first polymer layers between the substrate and the bulk polymer material, which are termed interphase. Standard methods have failed to completely characterize this interphase, because its properties change significantly over a few nanometers. Here we determine the spatially resolved adhesion properties of the interphase in polyelectrolyte multilayers (PEMs) by desorbing a single polymer covalently bound to an atomic force microscope cantilever tip from PEMs with varying thickness. We show that the adhesion properties of the first few layers (up to three double layers) is dominated by the surface potential of the substrate, while thicker PEMs are controlled by cohesion in between the PEM polymers. For cohesion, the local film conformation is the crucial parameter. This finding is generalized by utilizing oligoelectrolyte multilayer (OEM) as coatings and both hydrophilic and hydrophobic polymers as polymeric force sensors.

KEYWORDS: *thin polymer film, polyelectrolyte multilayer, atomic force microscopy, interphase, cohesion*
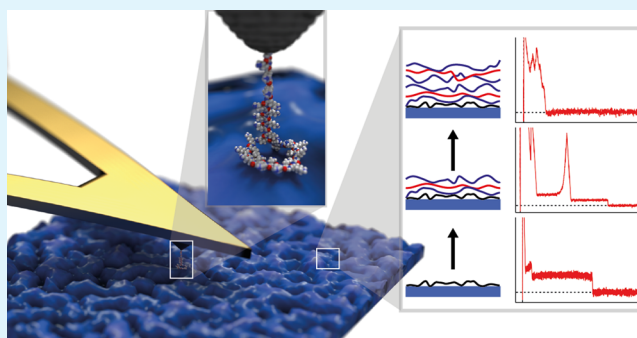
■ INTRODUCTION

Adhesion has become increasingly important in medical engineering applications. The fabrication of biocompatible devices such as anti-infective implants,[1−3] for example, seeks better understanding of adhesion in biosystems. Polymer coatings have often been used to change and control adhesion properties of substrates, in particular for the construction of nanoscopic components. Several studies covering that field use the surface force apparatus.[4] Atomic force microscopy (AFM) based single polymer detection has been used to delineate adhesion properties of single polymers on solid substrates in aqueous environment.[5,6] Altogether, these methods allowed a basic understanding of single polymers on solid substrates.

Here we address the question how the adhesion properties change once the substrate is coated with supported thin polymer films of varying thickness and composition. Those films change their properties from the interfacial layer close to the supporting substrate to the boundary layers having bulklike behavior.[7] The layer which differs in chemical composition or the conformational equilibrium from the bulk state is usually called the interphase.[8−10] This interphase likely has major implications on the adhesive properties of substrate coatings such as aging and self-healing.[7,11,12]

We use polyelectrolyte multilayers (PEMs) on silicon (Si) as model system. They can be prepared from sequential adsorption of oppositely charged polyelectrolytes onto a charged surface from aqueous solutions.[13−16] The layer-by-layer method enables the construction of ultrathin films with defined thickness, composition, and chemical functionalities. PEMs are known to be sensitive to external parameters such as salt concentration, type of salt, pH, and temperature during preparation as well as during application.[17−22] The basic mechanism for PEM stability and the adhesion mechanism for build-up are not fully understood. We use the following single polymer approach to detect and distinguish interface, interphase, and bulk region.

A polymer covalently bound to an AFM cantilever tip is pressed onto the PEM layer underneath with a force of several hundred piconewtons in aqueous environment.[23,24] Trigger values for the tip approaching the PEM are chosen in a way that only the top region is touched upon dwell on the PEM while the underlying Si substrate is not reached. The polymer is allowed to adsorb onto the surface with varying dwell time (see below). While retracting the AFM cantilever tip, the polymer successively desorbs (deadsorbs) from the surface. This method allows one to detect thin polymer adhesion properties with high spatial precision.

■ EXPERIMENTAL SECTION

Materials and Reagents. The linear poly(diallyl dimethyl ammonium chloride) (PDADMAC) was synthesized by free-radical polymerization. Details about the synthesis and the characterization are described elsewhere.[25,26] The molecular weight of PDADMAC is 135 kDa (PDI = 1.75) for high MW and 5 kDa (PDI = 1.5) for low MW polymer. Branched poly(ethylene imine) (PEI) and high MW poly(sodium-4 styrene sulfonate) (PSS) were obtained from Aldrich (Steinheim, Germany). The molecular weights were 750 kDa for PEI and 70 kDa (PDI = 2.5) for PSS. Low MW PSS (6 kDa, PDI < 1.2) was bought from Polymer Standard Service (Mainz, Germany); NaCl (99.9%) was purchased from Merck (Darmstadt, Germany).

Molecular force sensors were fabricated using poly(allylamine) (PAH, 65 kDa) and poly-L-lysine hydrobromide (PLL, 150−300 kDa) purchased from Sigma Aldrich. Poly(styrene-b-propylene sulfide), PS-X, was synthesized by sequential living anionic polymerization.[27] Standard SEC was performed with THF as the mobile phase (flow rate 1 mL·(min)$^{-1}$) on a SDV column set from PSS (SDV 1000, SDV 100000, SDV 1000000) at 30 °C. Calibration was carried out using PS standards (from Polymer Standard Service, Mainz, Germany). SEC measurement versus PS standard revealed M_n = 1.26 MDa, M_w = 1.34 MDa, PDI = 1.06.

Substrate Preparation. Poly(tetrafluorethylene) (PTFE) samples of 1.5 mm thickness were purchased from GM GmbH (Germany).

Diamond samples (HD) with [100] orientation and impurity concentrations lower than 1 ppm for nitrogen and 50 parts per billion (ppb) for boron were purchased from Element Six (U.K.). Diamond surfaces were cleaned in sulfuric acid prior to surface termination. Hydrogen surface termination was performed in a microwave-assisted hydrogen plasma as described in ref 28. Static contact angle measurements with pure H_2O showed a contact angle of 80°−90°.

Self-assembled monolayers (SAMs) of defined hydrophobicity were obtained by storing gold-coated glass slides (CrNi, 29 nm; Au, 129 nm) for 12 h in 2 mM 1-dodecanethiol dissolved in ethanol.[29,30]

Polyelectrolyte multilayers (PEM) were prepared on Si substrates purchased from AG Siltron (Korea). Prior to multilayer preparation, the substrates were treated with piranha solution (H_2SO_4/H_2O_2, 1:1, v/v) in order to remove organic contaminants and to activate the surface for polyelectrolyte adsorption. The polyelectrolyte multilayers were deposited on the Si wafers by the layer-by-layer technique. The substrates were immersed for 20 min (high MW polyelectrolytes) or 5 min (low MW polyelectrolytes) in polyelectrolyte solutions with a monomer concentration of 10^{-2} M in 0.1 or 0.5 M NaCl, respectively. The films were rinsed after each deposition step with pure H_2O. A precursor PEI layer was deposited from salt-free aqueous solution by dipping clean Si substrates for 30 min, then rinsing with pure H_2O. The presence of this precursor layer (thickness of 2 nm, Supporting Information, Table S1) enhanced the growth of the PEM while reducing heterogeneity effects.[31,32] The multilayers were dried in nitrogen stream after completion of the multilayer assembly. The prepared samples have 1, 1.5, 2, 2.5, 3, 4, 4.5, 14, and 14.5 double layers of (PSS/PDADMAC) prepared in 0.1 M NaCl and 0.5 M NaCl concentrations. The integer numbers correspond to PEMs with PDADMAC as outermost layer. For comparison pure Si substrates as well as PEI covered Si substrates were used.

AFM Cantilever Tip Functionalization. Si_3N_4 cantilevers (MLCT from Bruker AXS) were chemically cleaned and activated in an oxygen plasma. Amino-functionalized tip surfaces for the covalent coupling of polymers were obtained by using Vectabond reagent (Axxora, Germany) which is similar to (3-aminopropyl)triethoxysilane. The aminated cantilevers were immersed in a poly(ethylene glycol), PEG, with an appropriate mixture of the bifunctional and the monofunctional linker (Rapp-Polymere, Germany) solution in dry chloroform (>99.9%, Sigma-Aldrich) with 5 vol % triethylamine (Sigma-Aldrich) in order to provide coupling sites. For PLL and PAH, an ∼1:1500 mixture of homobifunctional PEG (PEG-(NHCO-C_2H_4-CONHS)$_2$) with NHS reaction sides (6 kDa, PDI = 1.07) addressing the amino groups and monofunctional PEG (CH_3O-PEG-NHS) with methoxy termination (5 kDa, PDI = 1.03) for passivation was used.

Then a polymer solution (max. 10 mg·mL^{-1} in 50 mM borate buffer, pH = 8.0) was taken for the coupling of the polymer for 90 min followed by rinsing in Tris buffer (10 mM, pH = 8.4).

For PS coupling, a 1:1500 mixture of heterobifunctional PEG (malhex-NH-PEG-O-C_3H_6-CONHS) with NHS and maleimide reaction sites (5 kDa, PDI = 1.03) addressing the sulfide group of PS and methoxy terminated monofunctional PEG (5 kDa, PDI = 1.03) was used. Afterward, a polymer solution (about 1 mg·mL^{-1} in chloroform) was used for an overnight coupling of PS. The functionalized cantilevers were rinsed and stored in chloroform until use in an experiment.

Covalent attachment to the AFM cantilever tip via flexible PEG linkers makes long measurements over a period of many hours with one and the same polymer on the different substrates and PEMs possible. This PEG linker (NHS or maleimide) covalently binds one end of a single probe polymer to the tip, and shifts the polymer away from the tip apex. This separates the adhesion related polymer−substrate interaction from the undesired contributions stemming from the unspecific interaction of the substrate with the tip material itself.[33] Furthermore, the methoxy-terminated PEG was mixed with the NHS or maleimide terminated PEG using a ratio that provides just very few binding sites for the PLL, PAH or PS respectively. In addition, the methoxy terminated PEG prevents unspecific readsorption of these polymer chains to the AFM tip. The quality of the functionalization has been controlled before and after PEM experiments using solid substrates such as PTFE. A clear single polymer event (plateau of constant force) and a narrow detachment length distribution are required to confirm good functionalization quality.

Single Molecule Force Spectroscopy (SMFS). The AFM measurements were performed with a MFP3D-SA (Asylum Research, Santa Barbara, CA) in a closed fluid cell. During indentation of the functionalized tip, the polymer adsorbed on the interface (dwell time of usually 1 s). The tip was then retracted with a constant velocity (e.g., 1 μm·s^{-1}). Force−extension traces were obtained from the deflection-piezopath signal as described elsewhere.[24,34] The traces were taken at least at three different positions on the interface. Each measurement contains at least 100 force−extension curves. The sampling rate was set to 5 kHz. The optical lever sensitivity was averaged over the first five and the last five retraction curves. The spring constant of each cantilever (values range between 10 and 50 pN·nm^{-1} was determined after the measurement by integrating over the power spectral density from 2.5 Hz to the local minimum between the first and the second resonance peak and by applying the equipartition theorem.[35−37]

The measured velocity-independent plateaus represent an equilibrium desorption process.[5] Each plateau corresponds to the desorption process of a single polymer. Evaluation was done with the program Igor Pro (Wavemetrics) and self-programmed procedures. The desorption force and the detachment length were determined from a sigmoidal fit to the plateau end. In case of multiplateaus,[38] the plateau indicating the desorption of the last polymer from the substrate was taken for evaluation. The errors given in the text and figures correspond to the standard deviation.

AFM Imaging. The MFP3D-SA AFM (Asylum Research, Santa Barbara, CA) was used in combination with AC 240 TS cantilevers (Olympus, Japan) with a force constant of about 1.8 N/m and a resonance frequency of 70 kHz at a scan rate of 0.5 Hz for intermittent-contact mode imaging.

Ellipsometry. For ellipsometric measurements a polarizer-compensator-sample-analyzer (PCSA) ellipsometer, Multiscope from Optrel GbR (Wettstetten, Germany) was used. The measurements were performed using a red laser light with wavelength of 632.8 nm and at incident angle of 70° (close to the Brewster angle of the Si/air interface) and 60° (solid/water). The sample environment was a homemade humidity chamber having a relative humidity sensor. The cell was made out of stainless steel with rubber sealed windows on the sides for the light guides connected to the laser and detector arms of the ellipsometer. For determination of thickness d and refractive index n of the multilayers from the measured Δ and Ψ values, the Elli software from Optrel was used together with a least-squares fit with
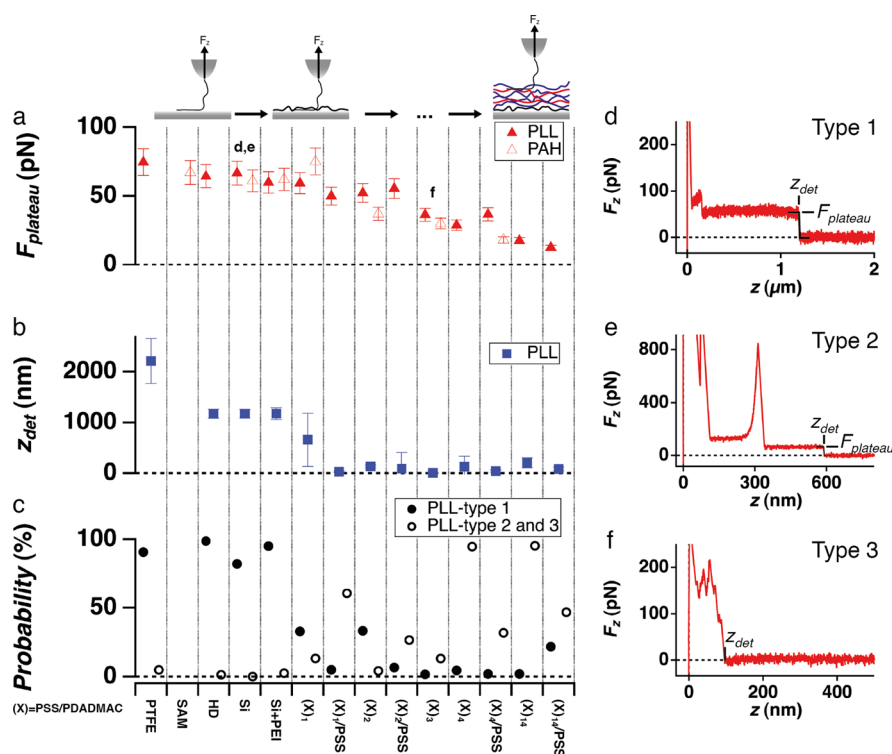
Figure 1. Interphase properties of PEM substrates: Single polymer desorption from PTFE, SAM, HD, Si, PEI covered Si (Si+PEI), (PSS/PDADMAC)$_1$, (PSS/PDADMAC)$_2$, (PSS/PDADMAC)$_3$, (PSS/PDADMAC)$_4$, and (PSS/PDADMAC)$_4$/PSS in H$_2$O. These PEMs were prepared in 0.1 M NaCl. (a) Plateau desorption force $F_{plateau}$ (type 1 and 2) for PAH and PLL as single polymer force sensor, (b) detachment length z_{det}, and (c) probability of curve type occurrence. (d) Example force−extension curve for PLL on Si for type 1 (plateau) and (e,f) example force−extension curve for PLL on (PSS/PDADMAC)$_3$ for type 2 (plateau and stretching) and type 3 (stretching and rupture only). Close to the substrate, an unspecific adhesion peak stemming from tip−substrate interaction is observed. Errors correspond to the standard deviation.

four-layer box model is used: (i) air ($n = 1$) or water ($n = 1.332$), (ii) multilayer, (iii) SiOx ($d = 1.5$ nm; $n = 1.4598$), and (iv) Si ($n = 3.8858$, $k = −0.020$). For each multilayer, both thickness and refractive index were fitted simultaneously without assuming a fixed refractive index. For multilayers with thickness less than 10 nm (1 and 2 double layers in 0.1 M NaCl and 1 double layer in 0.5 M NaCl), the Garnet equation[39] was used to cross check the thickness and refractive index. The thickness and refractive index obtained from the Garnet equation showed no significant difference from those given by the software.

RESULTS AND DISCUSSION

Effect of Number of Adsorbed PE Layers. PEMs of poly(sodium-4 styrene sulfonate) (PSS) and poly(diallyl dimethyl ammonium chloride) (PDADMAC) were prepared from aqueous electrolyte solution containing 0.1 or 0.5 M NaCl by the layer-by-layer method. The thickness in air and in H$_2$O was determined by ellipsometry (Supporting Information, Table S1). The swelling behavior has been characterized previously by ellipsometry and AFM imaging.[22]

Single molecule force spectroscopy (SMFS) data are taken in ultrapure H$_2$O with polyallylamine (PAH) or polylysine (PLL), as single polymer force sensor. Both are positively charged at neutral pH. We observe similar plateau desorption forces, depicted as $F_{plateau}$ in the following, for PTFE, hydrophobic (methyl) self-assembled monolayer (SAM), H-terminated diamond (HD) and Si in the absence of any polymer coating (Figure 1a). This is consistent with previous experiments on solid substrates,[5,6] which resemble a process close to equilibrium conditions. Therefore the dynamics between polymer and solid substrate occur on a much faster time

scale than the pulling velocity of our experiment.[24,27,34] The force drops to zero as soon as the polymer detaches.

In order to investigate the polymer interphase, we first added branched poly(ethylene imine), PEI, and then successive PEM layers according to the standard protocols mentioned above. The plateau desorption force $F_{plateau}$ already decreases after the first PSS/PDADMAC layer in a continuous manner to one-third of the initial value (Figure 1a). In addition, the detachment length z_{det}, defined as the point of the force−extension curves where the force falls to 0, immediately drops after the first PSS/PDADMAC layer (Figure 1b). In general, the plateau desorption force and detachment length decrease significantly with increasing number of (PSS/PDADMAC) layers.

Furthermore, two characteristic types of force−extension curves are observed. First, plateau desorption curves (here termed type 1) representing equilibrium events. Second, force−extension curves with nonlinear structures representing non-equilibrium stretching and rupture events (here termed type 3). Those resemble the force−extension curves for the rupture of single covalent bonds[40] or unfolding of secondary structures.[41,42] The obtained curves can be fitted using a wormlike chain model.[43−45] Type 2 force−extension plots comprise more complex curves including both plateau and nonlinear structures. A fourth type of curve shows no single polymer events at all (unspecific adhesion peak only). A transition from equilibrium to nonequilibrium desorption is observed for PEMs with more than one (PSS/PDADMAC) layer which is given by the ratio of plateau desorption curves (type 1, only equilibrium events) to all curves taken for a polymer substrate combination. Already

at four double layers, namely, (PSS/PDADMAC)$_4$, most of the traces show nonequilibrium events (type 3) as presented in Figure 1c. For 0.1−60 s of dwell time, the same dependencies are found (Supporting Information, Figure S1). Thus, a qualitative and quantitative change in polymer adhesion can be observed with increasing number of PE layers.

The quality of these observations is confirmed by scratching a (PSS/PDADMAC)$_{14}$ (prepared in 0.1 M NaCl) substrate and taking a force map with PLL as molecular force sensor in H$_2$O. Here plateau desorption curves (type 1) are only observed for the scratched region, that is, without polymer coating (Figure 2a,b). The intact PEM layer shows a strongly reduced
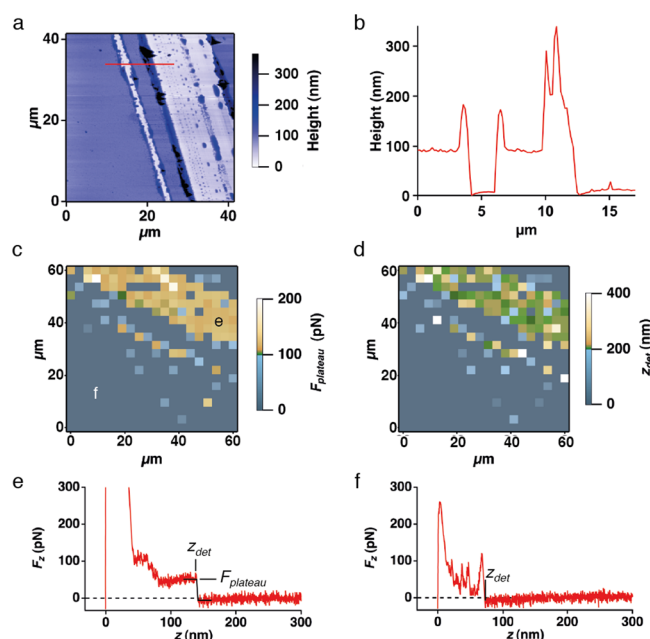

Figure 2. Effect of PEM layer on desorption behavior: (a) Intermittent contact AFM image in H$_2$O presenting an area being cut using a scalpel on (PSS/PDADMAC)$_{14}$ (prepared in 0.1 M NaCl). (b) Profile of the red line in (a). (c−d) Plateau desorption force F_{plateau} and detachment length z_{det} for a force map with PLL as sensor polymer on an area along the same cut given in (a). For nonequilibrium events (type 2 and 3), F_{plateau} and z_{det} are set to 0. Consistent with Figure 1, the PEM regions show rare of equilibrium desorption events. (e) F_z versus z curve from the scratch region with a desorption plateau. (f) F_z versus z curve taken on PEM region revealing sticky behavior in nonequilibrium (type 3). The data are obtained at a pulling velocity of 1 μm·s^{-1} and at a dwell time of 1 s.

unspecific adhesion peak, revealing the screening of substrate potential and the occurrence of nonequilibrium events, for one and the same single molecule force sensor. These results are confirmed on selected PEMs with 4 or 14 double layers probed by a polystyrene (PS-X) force sensor (Figure 3).

Furthermore oligoelectrolyte multilayer (OEM), built up by more than 10 times shorter PDADMAC and PSS are used. Those tend to be stiffer and show less coiling and thus lead to less interdigitation and thinner low-roughness films. The mobility of OEMs layers is 1 order of magnitude higher than for the long chain equivalents.[46,47] OEMs have the same tendency in single polymer equilibrium desorption (Figure 4) as for high molecular weight PEMs. As soon as the distances to the substrate become larger and the interpenetration rises, the plateau desorption force, detachment length, and occurrence of desorption plateaus decreases. Both plateau desorption force
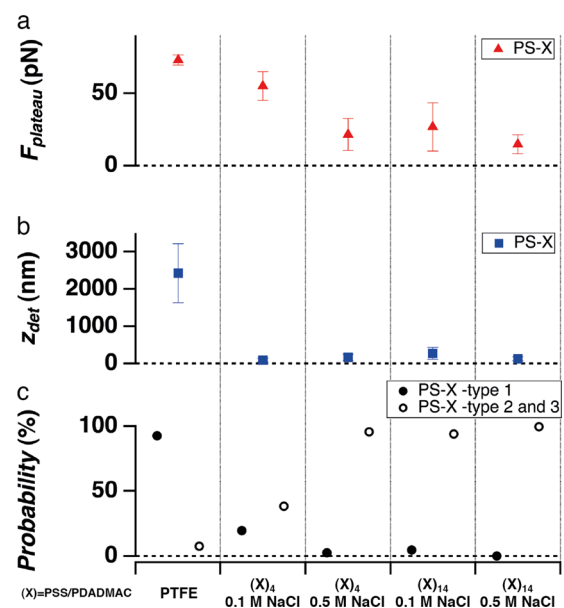
Figure 3. Desorption behavior of hydrophobic polymers: Single polymer desorption of PS-X from PTFE, (PSS/PDADMAC)$_4$ prepared in 0.1 M NaCl, (PSS/PDADMAC)$_4$ (0.5 M NaCl), (PSS/PDADMAC)$_{14}$ (0.1 M NaCl), and (PSS/PDADMAC)$_{14}$ (0.5 M NaCl). (a) Plateau desorption force F_{plateau} (type 1 and 2), (b) detachment length z_{det}, and (c) probability of curve type occurrence. These measurements are performed in H$_2$O with PS-X as sensor polymer using one and the same cantilever. Errors correspond to the standard deviation.
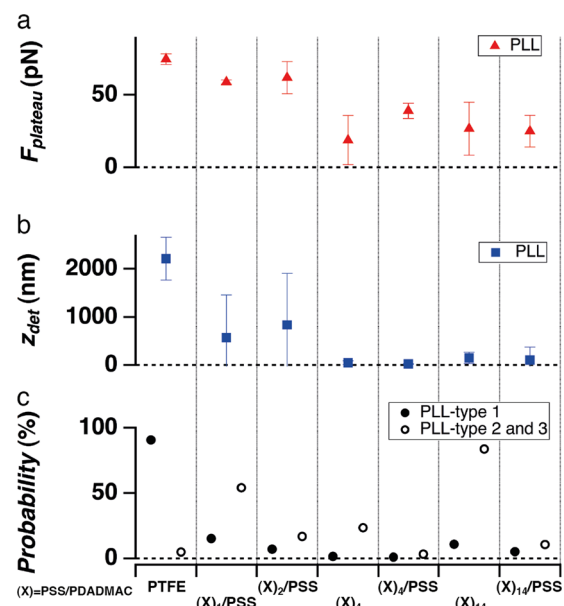

Figure 4. Desorption of short chain PEMs. Single polymer desorption from PTFE, (PSS/PDADMAC)$_1$/PSS prepared in 0.1 M NaCl, (PSS/PDADMAC)$_2$/PSS (0.1 M NaCl), (PSS/PDADMAC)$_4$ (0.1 M NaCl), (PSS/PDADMAC)$_4$/PSS (0.1 M NaCl), (PSS/PDADMAC)$_{14}$ (0.1 M NaCl), and (PSS/PDADMAC)$_{14}$/PSS (0.1 M NaCl). (a) Plateau desorption force F_{plateau} (type 1 and 2), (b) detachment length z_{det}, and (c) probability of curve type occurrence. These measurement are performed in H$_2$O with PLL force sensor using one and the same cantilever respectively. Errors correspond to the standard deviation.

and detachment length lead to this behavior after the second double layer. While still many type 1 events confirm the initial

6303

dx.doi.org/10.1021/am4013424 | *ACS Appl. Mater. Interfaces* 2013, 5, 6300−6306

detachment length, the type 2 and 3 events tend to show much shorter values. This reveals the broad z_{det} distribution in Figure 4b. The plateau probability is significantly reduced from the first double layer on. The higher stiffness of OEM chains could lead to reduced or even prevented interdigitation for one and two double layers. This underlines the importance of interdigitation for the type 2 and type 3 traces.

Molecular Model of PEM Desorption Behavior. The data are consistent with a model comprising two important adhesion mechanisms throughout the interface. In the first few layers (for thin PEMs), the substrate potential dominates the adhesion, but is already significantly screened after a few double layers. This is indicated by the equilibrium desorption plateaus, whose height, $F_{plateau}$, decreases by about a factor of 3 upon addition of the first three double layers. This goes hand in hand with the three zone model with a very small interphase of 2–3 double layers.[48] The shortening of the detachment length from the first (PSS/PDADMAC) layer hints toward a mechanism, where the polymer interacts with the PEM only partly. As soon as the PE layer fully screens the substrate potential (around three double layers), qualitatively different force extension traces are found, rendering the second adsorption mechanism more important. Already starting from the second double layer we obtain more and more nonequilibrium force−extension traces, resembling spikes (type 2 and 3) instead of plateaus (type 1). While the plateaus can be interpreted as desorption from the top layer of the PEM or the underlying Si substrate, either by being mobile on the PEM or in a zipper-like fashion[49] (Figure 5), the nonlinear force−extension curves of type 2 and
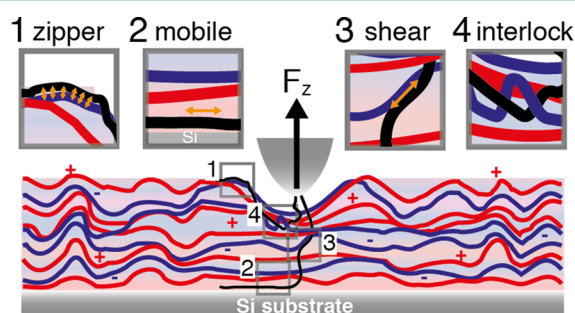
Figure 5. Schematic representation of single polymer desorption from PEMs: The tip pressing into the top layers of the PEM enables the tip bound polymer (black) to entangle at least partly into the PEM layer. Upon retraction the polymer shows four different motifs or combinations of these: (1) The polymer portion not entering the PEM reveals zipper-like detachment (zipper). (2) The polymer portion directly contacting the Si substrate leads to equilibrium desorption with high mobility. (1) and (2) result in plateaus in the force−extension curve (type 1). (3) The polymer part within the PEM is subject to shear and/or (4) to geometrical interlock events, both showing in nonlinear force−extension behavior (type 2 and 3).

3 have to be explained in a different manner. Here, sticky connections in between the tip attached polymer and the PEM coated substrate are necessary. As soon as the single tip attached polymer penetrates into the PEM it is geometrically trapped into the PEM mesh. The polymer then has to disentangle from the mesh when pulled in z direction under the exerted force F_z. The nonlinear force−extension (sticky) behavior can either be caused by intermolecular (electrostatic) bonds broken in a shear-like geometry[49] or by release of interlocks as indicated in Figure 5.

Properties of the Bulk Region Are Dominated by Cohesion. The behavior for four and more double layers is similar. Therefore, we interpret this as bulklike behavior and can restrict the interphase region to the first three (PSS/PDADMAC) double layers. Here, a crossover between substrate influence (equilibrium desorption) and cohesion dominance (nonequilibrium desorption) takes place.

Information on the global averaged conformation has been obtained before by neutron and X-ray reflectometry.[50−52] Our method is capable to add some information on the local molecular conformation of the tip bound polymer in contact with a substrate. This has been demonstrated in previous experiments on spider silk proteins/amyloids.[42,53,54] The first observation is that every force−extension trace looks different; therefore, the polyelectrolytes in the PEM do not have a unique conformation. Nevertheless, we observe some general trends. For few PE layers, we mostly obtain plateaus in the force extension trace, indicating that the polymer stays on top of the PEM with a high lateral diffusion coefficient, lacking entanglements. At around three double layers, we witness a transition to type 2 and 3 curves, which indicates some stronger local interactions. These are likely caused by mechanical interlock, as further discussed below. As such a transition is found for polymers of various composition, charge, and hydrophobicity, we believe that the polymers entangled with the PEM layer.

Role of Charges. The stability of PEMs is known to be due to two different effects: the entropy driven release of counterions (extrinsic charge compensation) and the enthalpic complexation between the oppositely charged PE layers (intrinsic charge compensation).[16,55] Our interpretation for the type 2 and 3 traces is a formation of complexes between the PEMs and tip bound polymers, which replace intra-PEM complexes between positively and negatively charged PEs. Upon desorption, these newly formed complexes have to be broken, causing the observed rupture peaks in the force−extension plots similar to cationic polymers desorbed from grafted anionic polyelectrolyte brushes.[56]

Although zeta-potential measurements demonstrate that the net charge of the surface changes after each monolayer adsorption step,[57−59] we observe similar behavior of (PSS/PDADMAC)$_4$ and (PSS/PDADMAC)$_4$/PSS, which are expected to carry opposite charges at the PEM top layer. This behavior could be explained by an interpenetration between adjacent layers which has previously been shown by neutron reflectometry measurements.[50−52]

The hydrophobic PS-X shows similar behavior as the PLL force sensor on PEMs with 4 and 14 double layers (Figure 3). In particular, nonequilibrium curves (type 2 and 3) are detected. Therefore, charges are not necessary to obtain sticky connections. The only remaining adhesion mechanism is geometrical interlock, which is discussed in more detail in the following.

Role of Geometrical Interlock. Our data is best explained by an entanglement of the polymer into the polymer film when the AFM cantilever tip pushes into the PEM with a force of several 100 pN (radius of curvature around 20 nm). The formation of entanglements between PE layers has previously been suggested due to X-ray reflectometry experiments.[60] As soon as the polymer is pulled out of the PEM, it has to find its way through the PE layers to be released. Breakage of interlocks is represented by desorption energies E_{des} (area under the force−extension curve) of the order of $1000 k_B T$ (Supporting

Information, Figure S2). Such a large value cannot be explained by unspecific interactions (e.g., screened charge interaction) only. Further evidence for interlocks comes from the observation that each force distance curve differs from the previous one, again requiring local interactions.

Varying the dwell time in contact with the PEM between 0.1 and 60 s does not show any change in plateau forces or in the probability of plateau occurrence (Supporting Information, Figure S1). PEMs of more than three double layers result in mostly type 3 curves with an increase in E_{des} (area under the force−extension curve) with increasing dwell time at short time scales between 0.1 and 1 s (Figure S2). Moreover, the distribution of E_{des} becomes broader with increasing dwell time which suggests some local conformational changes. Our picture is consistent with that of Ladam et al.[48] with a very small interphase of two to three double layers.

Another interesting observation is that the detachment length of the desorbed polymer is largely reduced on PEMs compared to solid substrates, already starting from the first double layer. This can be explained by partial incorporation of the AFM cantilever tip bound polymer into the PEM upon contact of the AFM cantilever tip. The remaining parts of the polymer stay on top of the PEM and detach as soon as the incorporated part is pulled off the PEM.

CONCLUSION

We determined the adhesion profile in supported PEMs by desorbing single polymers covalently bound to an atomic force cantilever tip from PEMs with varying thickness. A decrease in equilibrium desorption force, detachment length, and a transition from equilibrium to nonequilibrium desorption is observed within a few double layers. In thicker films, bulk behavior dominates, which is mainly given by the way a polymer entangles into the PEM. Through the interphase, we therefore have a crossover from substrate influence (equilibrium desorption) to cohesion dominance (nonequilibrium desorption). The charge of the polymer is not important for the general behavior, while its length affects the entanglements in the cohesion dominated bulk region.

In summary, we have been able to spatially separate the effect of substrate potential and local PE film conformation, which together determine the properties of the interphase. We anticipate that experiments of this kind will help in gaining a fundamental understanding of adhesion properties of other synthetic multicomponent systems as well as biological systems such as cartilage.[61]

ASSOCIATED CONTENT

Ⓢ Supporting Information

Overview of thickness values for different PEM layer compositions. Plateau force and probability for equilibrium desorption (type 1) for varying dwell time on PEM substrates as well as desorption energies for different dwell times on PEM substrates and varying indentation force are given. This material is available free of charge via the Internet at http://pubs.acs.org.

AUTHOR INFORMATION

Corresponding Author
*E-mail: thugel@mytum.de.

Present Address
∥S.D.: Kwame Nkrumah University of Science and Technology, Kumasi, Ghana.

Notes
The authors declare no competing financial interest.

REFERENCES

(1) Gristina, A. G. *Science* **1987**, *237*, 1588−1595.
(2) Hench, L. L.; Polak, J. M. *Science* **2002**, *295*, 1014−1017.
(3) Stickler, D. J. *Nat. Clin. Pract. Urol.* **2008**, *5*, 598−608.
(4) Maeda, N.; Chen, N. H.; Tirrell, M.; Israelachvili, J. N. *Science* **2002**, *297*, 379−382.
(5) Horinek, D.; Serr, A.; Geisler, M.; Pirzer, T.; Slotta, U.; Lud, S. Q.; Garrido, J. A.; Scheibel, T.; Hugel, T.; Netz, R. R. *Proc. Natl. Acad. Sci. U.S.A.* **2008**, *105*, 2842−2847.
(6) Geisler, M.; Balzer, B. N.; Hugel, T. *Small* **2009**, *5*, 2864−2869.
(7) Pukanszky, B. *Eur. Polym. J.* **2005**, *41*, 645−662.
(8) Sharpe, L. H. *J. Adhes.* **1972**, *4*, 51−64.
(9) Possart, W.; Kruger, J. K.; Wehlack, C.; Muller, U.; Petersen, C.; Bactavatchalou, R.; Meiser, A. *C. R. Chim.* **2006**, *9*, 60−79.
(10) Hartwig, A.; Meissner, R.; Merten, C.; Schiffels, P.; Wand, P.; Grunwald, I. *J. Adhes.* **2013**, *89*, 77−95.
(11) Hager, M. D.; Greil, P.; Leyens, C.; van der Zwaag, S.; Schubert, U. S. *Adv. Mater. (Weinheim, Ger.)* **2010**, *22*, 5424−5430.
(12) Xu, W.; Li, G. *Int. J. Solids Struct.* **2010**, *47*, 1306−1316.
(13) Decher, G.; Hong, J. D.; Schmitt, J. *Thin Solid Films* **1992**, *210*, 831−835.
(14) Decher, G. *Science* **1997**, *277*, 1232−1237.
(15) Hammond, P. T. *Curr. Opin. Colloid Interface Sci.* **1999**, *4*, 430−442.
(16) von Klitzing, R. *Phys. Chem. Chem. Phys.* **2006**, *8*, 5012−5033.
(17) Vanderschee, H. A.; Lyklema, J. *J. Phys. Chem.* **1984**, *88*, 6661−6667.
(18) Dubas, S. T.; Schlenoff, J. B. *Langmuir* **2001**, *17*, 7725−7727.
(19) Steitz, R.; Leiner, V.; Tauer, K.; Khrenov, V.; von Klitzing, R. *Appl. Phys. A: Mater. Sci. Process.* **2002**, *74*, S519−S521.
(20) von Klitzing, R.; Wong, J. E.; Jaeger, W.; Steitz, R. *Curr. Opin. Colloid Interface Sci.* **2004**, *9*, 158−162.
(21) Salomaki, M.; Tervasmaki, P.; Areva, S.; Kankare, J. *Langmuir* **2004**, *20*, 3679−3683.
(22) Dodoo, S.; Balzer, B. N.; Hugel, T.; Laschewsky, A.; von Klitzing, R. *Soft Materials* **2011**, *11*, 157−164.
(23) Ebner, A.; Wildling, L.; Zhu, R.; Rankl, C.; Haselgrubler, T.; Hinterdorfer, P.; Gruber, H. J. *Top. Curr. Chem.* **2008**, *285*, 29−76.
(24) Balzer, B. N.; Hugel, T. Single-Molecule Detection and Manipulation. In *Polymer Science: A Comprehensive Reference*; Matyjaszewski, K., Moeller, M., Eds.; Elsevier BV: Amsterdam, 2012; Vol. 2, pp 629−645.
(25) Ruppelt, D.; Kotz, J.; Jaeger, W.; Friberg, S. E.; Mackay, R. A. *Langmuir* **1997**, *13*, 3316−3319.
(26) Dautzenberg, H.; Gornitz, E.; Jaeger, W. *Macromol. Chem. Phys.* **1998**, *199*, 1561−1571.
(27) Balzer, B. N.; Gallei, M.; Hauf, M. V.; Stallhofer, M.; Wiegleb, L.; Holleitner, A.; Rehahn, M.; Hugel, T. *Angew. Chem., Int. Ed.* **2013**, *52*, 6541−6544.
(28) Hartl, A.; Garrido, J. A.; Nowy, S.; Zimmermann, R.; Werner, C.; Horinek, D.; Netz, R.; Stutzmann, M. *J. Am. Chem. Soc.* **2007**, *129*, 1287−1292.
(29) Bain, C. D.; Troughton, E. B.; Tao, Y. T.; Evall, J.; Whitesides, G. M.; Nuzzo, R. G. *J. Am. Chem. Soc.* **1989**, *111*, 321−335.
(30) Pirzer, T.; Geisler, M.; Scheibel, T.; Hugel, T. *Phys. Biol.* **2009**, *6*.

6305

dx.doi.org/10.1021/am4013424 | *ACS Appl. Mater. Interfaces* 2013, 5, 6300−6306

(31) Bosio, V.; Dubreuil, F.; Bogdanovic, G.; Fery, A. *Colloids Surf., A* **2004**, *243*, 147−155.

(32) Kolasinska, M.; Krastev, R.; Warszynski, P. *J. Colloid Interface Sci.* **2007**, *305*, 46−56.

(33) Geisler, M.; Pirzer, T.; Ackerschott, C.; Lud, S.; Garrido, J.; Scheibel, T.; Hugel, T. *Langmuir* **2008**, *24*, 1350−1355.

(34) Hugel, T.; Seitz, M. *Macromol. Rapid Commun.* **2001**, *22*, 989−1016.

(35) Hutter, J. L.; Bechhoefer, J. *Rev. Sci. Instrum.* **1993**, *64*, 1868−1873.

(36) Sader, J. E.; Larson, I.; Mulvaney, P.; White, L. R. *Rev. Sci. Instrum.* **1995**, *66*, 3789−3798.

(37) Pirzer, T.; Hugel, T. *Rev. Sci. Instrum.* **2009**, *80*.

(38) Scherer, A.; Zhou, C.; Michaelis, J.; Brauchle, C.; Zumbusch, A. *Macromolecules* **2005**, *38*, 9821−9825.

(39) Wong, J. E.; Rehfeldt, F.; Hanni, P.; Tanaka, M.; von Klitzing, R. *Macromolecules* **2004**, *37*, 7285−7289.

(40) Grandbois, M.; Beyer, M.; Rief, M.; Clausen-Schaumann, H.; Gaub, H. E. *Science* **1999**, *283*, 1727−1730.

(41) Rief, M.; Gautel, M.; Oesterhelt, F.; Fernandez, J. M.; Gaub, H. E. *Science* **1997**, *276*, 1109−1112.

(42) Geisler, M.; Xiao, S. B.; Puchner, E. M.; Grater, F.; Hugel, T. *J. Am. Chem. Soc.* **2010**, *132*, 17277−17281.

(43) Hugel, T.; Grosholz, M.; Clausen-Schaumann, H.; Pfau, A. s.; Gaub, H.; Seitz, M. *Macromolecules* **2001**, *34*, 1039−1047.

(44) Puchner, E.; Gaub, H. *Curr. Opin. Struct. Biol.* **2009**, *19*, 605−614.

(45) Li, H. B.; Cao, Y. *Acc. Chem. Res.* **2010**, *43*, 1331−1341.

(46) Nazaran, P.; Bosio, V.; Jaeger, W.; Anghel, D. F.; von Klitzing, R. *J. Phys. Chem. B* **2007**, *111*, 8572−8581.

(47) Micciulla, S. A study on the effect of salt concentration on self-assembly and surface properties of oligoelectrolyte multilayers. Masters Thesis, Technische Universität, Berlin, 2011.

(48) Ladam, G.; Schaad, P.; Voegel, J. C.; Schaaf, P.; Decher, G.; Cuisinier, F. *Langmuir* **2000**, *16*, 1249−1255.

(49) Strunz, T.; Oroszlan, K.; Schafer, R.; Guntherodt, H. J. *Proc. Natl. Acad. Sci. U.S.A.* **1999**, *96*, 11277−11282.

(50) Schmitt, J.; Grunewald, T.; Decher, G.; Pershan, P. S.; Kjaer, K.; Losche, M. *Macromolecules* **1993**, *26*, 7058−7063.

(51) Losche, M.; Schmitt, J.; Decher, G.; Bouwman, W. G.; Kjaer, K. *Macromolecules* **1998**, *31*, 8893−8906.

(52) Jomaa, H. W.; Schlenoff, J. B. *Macromolecules* **2005**, *38*, 8473−8480.

(53) Karsai, A.; Martonfalvi, Z.; Nagy, A.; Grama, L.; Penke, B.; Kellermayer, M. S. Z. *J. Struct. Biol.* **2006**, *155*, 316−326.

(54) Alsteens, D.; Ramsook, C. B.; Lipke, P. N.; Dufrene, Y. F. *ACS Nano* **2012**, *6*, 7703−11.

(55) Joanny, J. F.; Castelnovo, M.; Netz, R. *J. Phys.: Condens. Matter* **2000**, *12*, A1−A7.

(56) Spruijt, E.; van den Berg, S. A.; Cohen Stuart, M. A.; van der Gucht, J. *ACS Nano* **2012**, 5297−5303.

(57) Adusumilli, M.; Bruening, M. L. *Langmuir* **2009**, *25*, 7478−7485.

(58) Caruso, F.; Lichtenfeld, H.; Donath, E.; Mohwald, H. *Macromolecules* **1999**, *32*, 2317−2328.

(59) Enrique Moya, S.; Iturri Ramos, J. J.; Llarena, I. *Macromol. Rapid Commun.* **2012**, *33*, 1022−1035.

(60) Lvov, Y.; Decher, G.; Mohwald, H. *Langmuir* **1993**, *9*, 481−486.

(61) Han, L.; Dean, D.; Daher, L. A.; Grodzinsky, A. J.; Ortiz, C. *Biophys. J.* **2008**, *95*, 4862−4870.